RESEARCH ARTICLE | FEBRUARY 27 2024

Two operating modes for outer hair cells and implications for cochlear tuning

Jonathan Ashmore

AIP Conf. Proc. 3062, 050001 (2024)
https://doi.org/10.1063/5.0189846

Two Operating Modes for Outer Hair Cells and Implications for Cochlear Tuning

Jonathan Ashmore

UCL Ear Institute and Dept of Neuroscience, Physiology and Pharmacology London WC1E 6BT, UK

j.ashmore@ucl.ac.uk

Abstract. The role of cochlear outer hair cells (OHCs) in mammal hearing is compromised by the 'RC time constant problem'. The issue arises because if the cells are to operate at high acoustic frequencies conventional voltage driven 'electromotility' is low pass filtered by the cell membrane. By synthesising a description of the OHC as a piezoelectric actuator and its position between resonant basilar and tectorial membranes it is shown that sharp tuning can arise at high frequency if prestin/SLC26A5 is dynamically tensioned. The model predicts an imaginary (dissipative) component to the OHC capacitance as well as two distinct frequency tuning curve (ftc) shapes: a near symmetrical ftc at low CF, and a low frequency 'tail' on the more sharply tuned high CF ftcs

INTRODUCTION

The outer hair cells (OHCs) of the mammalian cochlea play an essential role amplifying incoming sound and making normal hearing possible. The evidence stems from a variety of different experiments but most significantly from the observation that OHCs elongate and shorten when their membrane potential is changed, from the cells' position in the organ of Corti and from evidence that the gene for prestin/SLC26A5 determines cochlear sensitivity (reviewed for example in [1]). The role of outer hair cells and the requirement for an actuator molecule prestin/SLC26A5 thus seems sufficient for cochlear performance over the entire acoustic range. Nevertheless direct measurement of OHC movement both in vitro [2] and in vivo from basilar membrane measurements of gerbil OHCs [3] highlights a long term concern that the OHC membrane acts like a lowpass filter of voltage, a problem which has come to be known as the 'RC-time constant problem' [4]. One escape from the paradox is to propose that the OHC RC time constant, τ, continues to decrease towards the basal end of the cochlea and so mitigate the effect, at least for measurable time scales imposed by patch clamp recording [5]

A line of modelling studies of single OHCs, based on the properties of prestin's non-linear capacitance, suggest that OHCs are capable of injecting power at the higher end of the acoustic range [6] [7] [8]. The ideas owe much to the suggestion that mechanical loading extends the OHC bandwidth [9].The present work combines prestin-dependent properties of the OHCs with a simple 1D model of cochlear micromechanics to investigate how such a scheme might enhance cochlear tuning. In the present case, the varying geometry of the organ of Corti along the cochlea and the precise configuration of hair cell excitation will, to first approximation, be neglected. The inclusion of such geometric factors has been considered elsewhere [10] in a model on which some the present considerations are based**.**

The governing set of equations for the 1-D amplitude motion, ξ, of the basilar membrane (BM) is given by a set of coupled oscillators embedded in fluid,

$$\sum_j \left(G_{ij} + m\delta_{ij} \right) \ddot{\xi}_i + \ h_i \dot{\xi}_i + \ k_i \xi_i = -f_i(\xi, t) \tag{1}$$

represented here by the discretised version (where the dots signify time derivative). The BM amplitude ξ is adopted to distinguish it from longitudinal cochlear position, x, discretely indexed as i. The term fi (ξ,t), is the local forcing

Nonlinearity and Hearing: Advances in Theory and Experiment
AIP Conf. Proc. 3062, 050001-1–050001-8; https://doi.org/10.1063/5.0189846
Published by AIP Publishing. 978-0-7354-4844-5/$30.00

term at position i. The parameter k = k(x) is the stiffness of the partition at each point x along the cochlea, h=h(x) is a viscosity parameter, accounting for both the local fluid viscosity in scala media as well as that arising in the subtectorial space.

Although m=m(x) in Eqn (1) is described conventionally as a partition mass, the additional term G(x,x') is included as non-local fluid mass term and performs the function of fluid coupling. It is the discretised hydrodynamic Green's function G(x,x') for the problem and can be calculated from a knowledge of the dimensions of the cochlear fluid volumes [11], [12]. For simplicity the total point mass will be termed m in what follows. The problem term in Eqn (1) is the damping hi dξ/dt that leads to dissipative energy loss, reducing sharp tuning of the BM. It includes any viscosity contributions from cells of the organ of Corti as well as the viscous forces at the interface between the TM and the reticular lamina. OHCs enter the description by the addition of a second forcing term to the right hand side, an 'undamping' term $f_{i,OHC}$ [13].

$$f_i(\xi, t) \rightarrow f_i(\xi, t) + f_{i,OHC}(\xi, t)$$

RESULTS

Cochlear micromechanics with OHC feedback

To calculate f_{OHC} at each point when the OHCs are part of a feedback loop it is necessary to include the effects of the forces arising from the OHCs and any response of prestin/SLC26A5. A simple feedback scheme of the OHCs sandwiched between a resonant tectorial membrane tectorial (TM) and a resonant basilar membrane (BM) (Fig 1) will be used and closely follows the treatment elsewhere [10].

Fig 1A shows a point hair cell model with two resonant structures. Both resonant structures, the TM and the BM are referenced to the modiolus. The equations for the movement, ξ, of the BM, and y for the TM are thus (dropping the place indices) are

$$H_{BM}\xi = -f_s - f_{OHC} \quad ; \quad H_{TM}y + f_{OHC} = 0 \tag{2a,b}$$

where fs is the stapes forcing term applied as a result of sound entering at the basal end, and f_{OHC} is the combined force due to OHCs and the organ of Corti. In Fourier space, with $\omega = 2\pi f$ and $j = \sqrt{-1}$, the operators are: $H_\alpha(\omega) = k_\alpha\left(1 + j\,\bar{\omega}_\alpha/Q_\alpha - \bar{\omega_\alpha}^2\right)$ where $\bar{\omega}_\alpha = \omega\sqrt{m_\alpha/k_\alpha}$; and $Q\alpha = \sqrt{m_\alpha k_\alpha}/h_\alpha$ are best frequency and quality factors respectively for α = BM or TM.

If the OHC electromotility is absent the system is purely passive; the organ of Corti itself couples the TM and the BM with an effective force $Z_{OHC}(y - \xi)$ where ZOHC is the impedance of the OHC including the organ of Corti. In this case Eqn 2 shows that the BM will experience a force of

$$f_{OHC} = -H_{TM}\,y = -\frac{H_{TM}\,Z_{OHC}}{(H_{TM} + Z_{OHC})}\xi \tag{3}$$

both the OHCs and the TM will behave like mechanical impedances in series. In general the force f_{OHC} will be a function of frequency and the BM mechanics will reflect loading by the TM even in this passive case.

OHCs as piezoelectric actuators

The OHC can be described as a 1D piezoelectric device expanding its length by two (linearised) equations [7]:

$$\delta S = c\delta T + d_{31}\,\delta V\,; \quad \delta Q = d_{13}\delta T + \varepsilon\delta V \tag{4a,b}$$

where δS (=δL/L) is the incremental length (or strain), and δQ is the charge displaced when the device is subject to increments in the tension T and voltage V around the equilibrium. The voltage dependent parameters d_{31} and d_{13} characterise the piezoelectricity (the subscripts indicating the tensor nature of the parameters). The parameter c is the compliance (inverse stiffness) of the cell. The equations can be seen as modifications of Hooke's Law and charge storage by a capacitance ε , both terms of which can be absorbed into the passive mechanics before any OHC feedback is included.

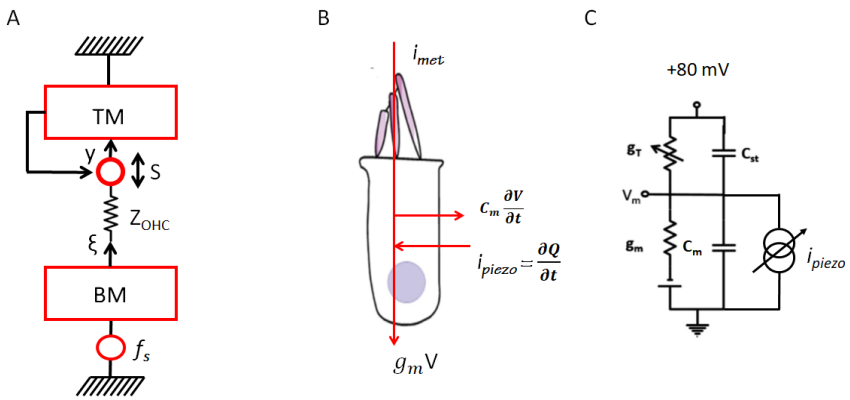

FIGURE 1 A, a 1-D model with the OHC driven by feedback from the TM. Note the direction in which the BM and TM directions are defined relative to the modiolar reference points. B, model of the OHC: transducer current i_{met}, C_m the membrane capacitance. i_{piezo} the displacement current produced by OHC tension, arising from anion and intrinsic charge movement associated with prestin/SLC26A5. C, the equivalent circuit with i_{piezo} appearing as a tension dependent current in addition to the current through the m.e.t. conductance g_T

Hair cell transduction

Deflection of the hair bundle activates a transduction current i_{met} which drives the membrane voltage (Fig 1B,C)

$$i_{met} = g_m V + C_m \frac{dV}{dt} + i_{piezo} \tag{5}$$

The first two terms $g_m V$ and C_m dV/dt are the conventional currents flowing through the membrane conductance and the total membrane capacitance (Fig 1B,C). The conventional RC time constant is $\tau = C_m/g_m$ An additional term is included in Eqn 5: $i_{piezo} = \frac{\partial Q}{\partial t}$ represents the current arising in OHCs due to charge movement when prestin/SLC26A5 is deformed. This displacement current can be observed experimentally [7], [14]; [15]. The transducer current, i_{met}, is a nonlinear function of displacement but can be linearised for small signals as $i_{met} = -\beta y$ in the convention of Fig 1A

As the OHC changes length, some of the displacement change is taken up by the strain change S of the cell. The force produced by the cells between the BM and TM will therefore be Z_{OHC} (y-ξ – δS). Other (passive) mechanical components of the organ of Corti, in parallel with the OHCs, can be absorbed into the OHC spring impedance Z_{OHC}. As a result, algebraic combination of Eqns 4 and 5 in the Fourier domain allows the force f_{ohc} to be written as the sum of two terms

$$f_{OHC} = -H_{TM} K \frac{1+ j\omega\tau(1-K\gamma H_{TM})}{(1-\alpha+ j\omega\tau(1-K\gamma H_{TM})} \xi + \gamma H_{TM} K \frac{j\omega\tau(H_{BM}-KH_{TM})}{(1-\alpha+ j\omega\tau(1-K\gamma H_{TM}))} \xi \tag{6}$$

where $\boldsymbol{\alpha} = K d_{31}\beta/g_m$, $\boldsymbol{\gamma} = \frac{d_{31}d_{13}}{C_m}$ and $K = \frac{Z_{OHC}}{H_{TM} + Z_{OHC}}$. Eqn 6 reduces to Eqn 3 when d_{31}=0, i.e. no OHCs.

The piezo parameters d_{31}, d_{13} have been measured in guinea pig OHCs [7]; the m.e.t. slope β and the conductance g_m have been measured in gerbil [5] so that we can estimate $d_{31}\beta/g_m$ ~ 5.3 for a 25 μm OHC and thus 1-α<0. This implies that the force f_{OHC} is real and positive in the low frequency limit (ωτ<<1). The force therefore acts as negative feedback and increases the stiffness of the BM at low frequencies.

The full expression for the force in Eqn 6 depends on γ, a coupling parameter that is the product of both OHC piezoelectric parameters, d_{31} and d_{13} Since both parameters are voltage dependent, the value of the coupling parameter γ can also depend on the membrane potential V of the OHC, opening the possibility of dynamic tuning of cochlear force feedback and sensitivity. It should be noted that the expression, Eqn 6, reduces to the TM loading of the BM

(Eqn 3) when d_{31} =0 (no electromotility); when d_{13} =0 (i.e. no tension sensitivity of prestin) Eqn (6) reduces to the expression given by Geisler and Shan [16] [10].

The second term in Eqn 9 vanishes when γ =0 (i.e. when i_{piezo} is not included) but depends explicitly on the BM impedance H_{BM}. Notably the term also depends on the product of the BM and TM stiffnesses and so can compensate for the increasing stiffness of BM towards the basal end of the cochlear end

Effective capacitance of OHCs

The denominators in Eqn 6 exhibit an effective time constant $\tau' = R_m C_{eff} = \tau(1 - K\gamma H_{TM})$. It depends on the piezo electric parameter γ and the OHC and TM impedances. If H_{TM} is real (i.e. no viscosity) then the time constant τ'can become arbitrarily small for suitable parameter choice or even negative [6]. If the TM has viscosity, as would be the case if it were a resonant structure, then τ', and hence C_{eff}, can take on complex values as well. This is equivalent to exhibiting dissipative losses by the OHC capacitance. Such results have been reported for OHC macropatches [17]. The results are shown in Figure 2.

Since $\gamma=d_{31}d_{13}/Cm$ depends on the square of the piezo parameters, Ceff measured when the OHC is loaded may have a stronger voltage dependence than that of the isolated cell's nonlinear capacitance. This conclusion can be experimentally investigated.

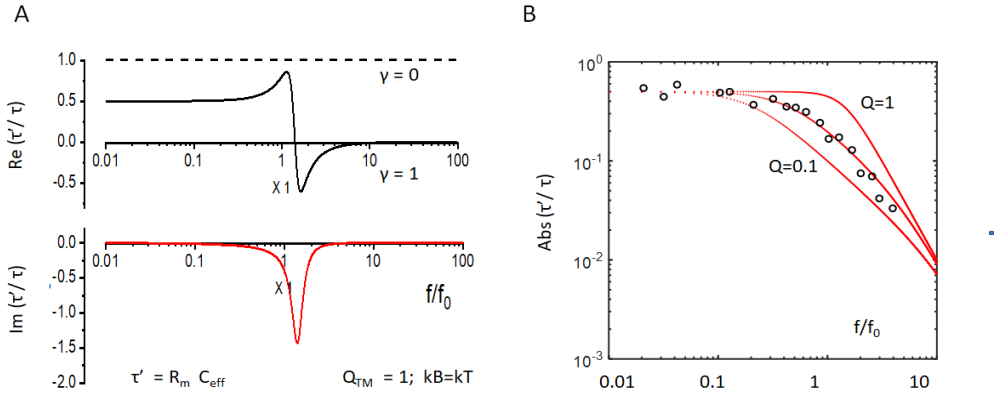

FIGURE 2. Effective OHC time constant τ'. A, real and imaginary parts of the function $\tau' = \tau(1 - K\gamma H_{TM})$ with $k_{ohc}=k_{TM}$ γ as shown. B, Absolute magnitude of effective capacitance $C_{eff} = \tau'/R_m$. circles, data from single OHC patches as in [14] with f_0 = 12 kHz. The curve fits a resonant system H_{TM} with high damping (Q=0.5) compatible with data from OHC membrane patches..

Threshold cochlear tuning curves

Although the parameter space is large, it is possible to see how the extra term contributes to tuning. Consider the simple case where both the BM and the TM are resonant structures with the same corner frequencies. The real part of the second in Eqn 6 term will vanish when Re $(H_{BM} - KH_{TM}) = 0$ or equivalently when the BM impedance is matched by the impedance of the TM and OHC in series. Hence we choose for simplicity $Z_{OHC} = k_{ohc}=k_{TM} =2\ k_{BM}$. Thus the impedance of the TM and OHC together match that of the BM at low frequencies. In this case f_{ohc} is purely imaginary and proportional to the negative viscous damping of the BM, with a correction for any resonant effects dependent on the TM. The gain is determined by the piezo parameter γ. The cancellation may be imperfect for it will be modified by the presence of the non-local Green's function coupling term G(x,x') in Eqn 1.

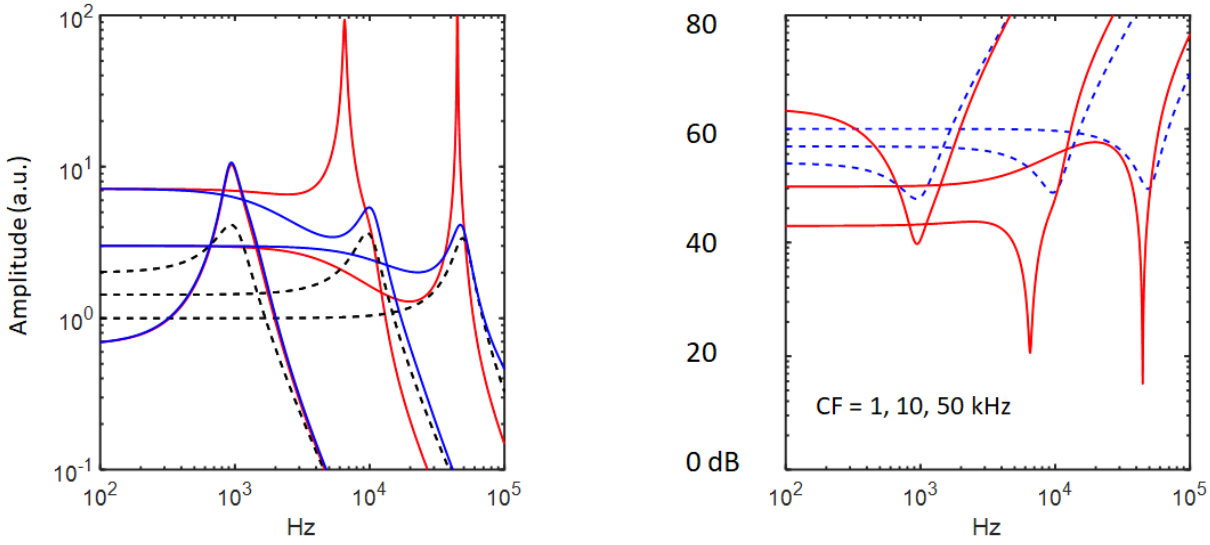

FIGURE 3. Indicative tuning curves for three cochlear positions inferred from Eqn 6. Left, BM tuning; Right inferred frequency tuning curves, with a scale given in dB. Black dashed line, the transfer function of the BM alone; red, transfer function of the BM with effects of f_{ohc} (i.e. $1/(H_{BM} - f_{ohc})$; blue, transfer function of BM with f_{ohc}, but with γ=0. The positions correspond to apical 1 kHz, mid-10 kHz and basal 50 kHz locations. The underlying tuning is established by the passive mechanics of the BM with only small changes in the mechanical Q_{3dB} of the BM. The range of parameters chosen were (kHz, $d_{31}\beta/g_m$, γ): (1, 2.5, 0.8); (10, 4..5, 3,2); (50, 5, 3,3)

With suitable choice of parameters, the effect of OHC enhancement over the passive BM tuning can reach 40 dB or more . Fig 3 shows the that characteristically sharp tuning curve can be obtained for a resonant TM. It can also be obtained for a non-resonant TM, the main difference being that the resonant TM generates a notch on the low frequency side of the high CF tuning curve. The mechanical power dissipation by this system of OHCs will be $\dot{\xi} f_{OHC}(\xi)$. A critical role is played by $\boldsymbol{\gamma} = d_{31}d_{13}/C_m$ which determines not only the mechanical undamping in Eqn 6, but also determines the effective imaginary capacitance of the OHC (i.e. dissipative effects) though the expression for $\tau' = R_m C_{eff}$.

DISCUSSION

Below a cut-off frequency determined by the cell membrane time constant, OHC 'electromotility' provides positive feedback. Above such cut-off frequency the results show that there is also a regime where the charge flowing through the prestin, not just the m.e.t. channel, can contribute to feedback and enhancement of the BM motion.

Before the identification of prestin/SLC26A5 the models of OHC function depended upon a phenomenological fit to the data rather than a traceable molecular mechanism. OHC feedback was required to be specified up to a gain factor, adjusted to obtain agreement enhancement of the BM tuning [18]. Piezoelectric descriptions reduce that ambiguity by basing the feedback on experimentally determined cellular data. The piezoelectric OHC properties are energy dependent and the mechanical power dissipation at each point is $\dot{\xi} f_{OHC}(\xi)$. Physically this can be thought of as either viscous losses of the protein-lipid environment, or viscous loading of the whole OHC. It has also been argued that such mechanisms might arise from energetically favoured binding of the anionic charge in prestin [19]. The source of the energy, however, is the potential across the cell membrane, maintained by the endocochlear potential, through which anions or intrinsic charges of prestin move.

It is noticeable that when measured in isolated OHCs, the piezo coefficients d_{13}, d_{31} are not completely equal. Charge displacement vs force curves shows that $d_{13} < d_{31}$ particularly at the most sensitive range (see Fig 5B in [7]). This may indicate some pre-existing degree of dissipation built into the OHC prestn/SLC26A5 system.

The model described here does not include any non-linearity since all parameters have been linearised around the operating point. The incorporation of any non-linear component to generate distortion products depends upon the inclusion of the mechano-electric transduction I-X curve. The voltage dependence of the prestin is not sufficient to

contribute a significant nonlinearity for small signals. One time domain model that does produce distortion products is that of Nobili and Mammano, [18]. The approach there was to expand the first term of Eqn 6 to first order in β and then identify β as the I-X function under assumptions that simplify Z_{OHC} and H_{TM}. The full set of cochlear equations can then be numerically computed in the time domain as the m.e.t. nonlinearity enters in a tractable form. The price of the expansion is the introduction of a variable gain parameter which substitutes for the positive feedback afforded by experimental parameters in Eqn 6.

Two cochlear tuning regimes

The development of the model in Fig 3 shows that at low frequencies the effect of i_{piezo} can largely be ignored and the system exhibits positive feedback driven by the transduction current. This is a conventional electromotility model. In this case the tuning is quite broad. At high frequencies, beyond the membrane cut-off, the system dynamics changes and the tuning becomes sharper. It has been argued that at least up to 20 kHz, the membrane time constant τ continues to fall and so that the low frequency cut off might never be approached and sufficient membrane potential change exists to drive a voltage sensitive prestin [5]. Although attractive, there are technical and bandwidth limitations to testing this proposition further using conventional patch clamp techniques.

A feature of auditory tuning curves often remarked upon is that there are discontinuities in the sharpness of tuning (the Q values) as well as the high frequency slopes at the measured CFs continue to rise [20]. The discontinuities distinguish tuning curves with CFs above or below 5 kHz. In addition, tuning curves with high CFs have a noticeable low frequency 'tail' or plateau in a wide variety of mammalian species (see for example [21] [22]). The treatment above suggests that the origin of such features may be the two modes of any OHC contribution to BM mechanics (Eqn 6). These characteristics are shown in Figure 3B where the inverse of the transfer curves ($1/(H_{\mathbf{BM}} - f_{OHC})$ have been plotted as very oversimplified indication of the threshold frequency tuning curves, but which neglects further nonlinearities from hair cell transduction, coupling between cochlear sections and any of the known non-linearities of synaptic transmission.

CONCLUSION

Although the effect of fluid coupling has been ignored in this simple point model, the results indicate semi-quantitively the curves that would be obtained in the intact cochlea. The low CF tuning curve is broader than for high CF; the high CF curve shows a low frequency plateau which is due mainly to the contribution of the m.e.t. driven OHC motility. The contribution to low frequency responses comes from RC-time constant limited motility of the OHC; the contribution to high frequency components of the curve arising from the charge movement inherent in the movement of anions at the cytoplasmic vestibule of prestin/SLC26A5 as well as charge reorganization of the protein. Recent cryo-e.m. structures of SLC26A5 may help to resolve the precise molecular mechanisms underlying such dynamics [23] [24].

Time domain models, including the effects of wave propagation in the cochlear duct, are computationally harder to implement but the solutions defy easy analytical expression. Eqn 6 does admit a time domain formulation but necessarily involves adding the effect of the Green's function G(x,x'). It is unfortunate that the resulting computational complexity often obscures the underlying biophysics even though such models can automatically include the non-linear consequences of hair cell transduction including distortion products and compressive behaviour of the mechanics away from a linear threshold. The present highly simplified treatment can provide a framework in which the full time-dependent solution can be understood.

ACKNOWLEDGEMENTS

I thank Robert Fettiplace for comments on an earlier version of this work.

COMMENTS & QUESTIONS

Jont Allen: You warned me! So the experiment that I think will prove whether you are right or wrong about this is to use low side suppression on the basilar membrane and to use it in your model. On the basilar membrane, low side suppression thresholds are 20 dB higher or more than in the neuron. I think that that the same logic applies to this case.

Author (J. Ashmore): I don't have proper answer for you. All I can say is that this is a linear model and moving from the frequency domain to the time domain is much more problematic (with at least two steps of non-linear processing, the mechano-electric transduction and the synaptic transmission, before the nerve thresholds are determined), but if you can do that then you may end up with some of the nonlinear effects that you are describing.

Jont Allen: Indeed that is the case. Sondhi and I have a whole bunch of papers on exactly that topic. I also have a piezo electric model of the hair cell based on Kuni Iwasa's work.

Author (J. Ashmore): Thank you. I'm just trying to avoid too much complexity in the mathematics and to provide a simple framework that most neurobiologists can appreciate.

Chris Bergevin: A quick comment and a question. If I'm not mistaken I think there are three components to a mammalian auditory nerve fiber response. At very high frequencies, at high levels, I think you can also see a plateau. But can you also comment on the mouse audiogram? I always say to students that the mouse cannot hear below 1 kHz, but from an evolutionary point of view this seems really dumb! Do they really not hear below 1kHz since that's going to be a huge evolutionary disadvantage?

Author (J. Ashmore): Well, that is what the audiogram indicates, unless there is some sort of subharmonic detection. There are very strong evolutionary arguments to suggest that high frequency hearing came first and lower frequency hearing is a bolt-on. Mammals (and their evolutionary antecedents) have been around for 300 myr, long before their radiation when the dinosaurs became extinct, but I'm afraid that evolutionary speculation usually stumps everybody!

REFERENCES

1. J. Ashmore, *Outer Hair Cells and Electromotility*, Cold Spring Harb Perspect Med **9**, (2019).
2. J. Santos-Sacchi, K. H. Iwasa, and W. Tan, *Outer Hair Cell Electromotility Is Low-Pass Filtered Relative to the Molecular Conformational Changes That Produce Nonlinear Capacitance*, J. Gen. Physiol. **151**, 1369 (2019).
3. A. Vavakou, N. P. Cooper, and M. van der Heijden, *The Frequency Limit of Outer Hair Cell Motility Measured in Vivo*, Elife **8**, (2019).
4. P. Dallos and B. N. Evans, *High-Frequency Motility of Outer Hair Cells and the Cochlear Amplifier*, Science **267**, 2006 (1995).
5. S. L. Johnson, M. Beurg, W. Marcotti, and R. Fettiplace, *Prestin-Driven Cochlear Amplification Is Not Limited by the Outer Hair Cell Membrane Time Constant*, Neuron **70**, 1143 (2011).
6. K. H. Iwasa, *Negative Membrane Capacitance of Outer Hair Cells: Electromechanical Coupling near Resonance*, Sci Rep **7**, 12118 (2017).
7. X. X. Dong, M. Ospeck, and K. H. Iwasa, *Piezoelectric Reciprocal Relationship of the Membrane Motor in the Cochlear Outer Hair Cell*, Biophysical Journal **82**, 1254 (2002).
8. R. D. Rabbitt, *The Cochlear Outer Hair Cell Speed Paradox*, PNAS **117**, 21880 (2020).
9. D. C. Mountain and A. E. Hubbard, *A Piezoelectric Model of Outer Hair Cell Function*, J Acoust Soc Am **95**, 350 (1994).
10. C. D. Geisler, *A Realizable Cochlear Model Using Feedback from Motile Outer Hair Cells*, Hear Res **68**, 253 (1993).
11. Allen and Sondhi, *Cochlear Macromechanics: Tiem Domain Solutions*, J. Acoust. Soc. Am. **66**, 123 (1977).
12. F. Mammano and R. Nobili, *Biophysics of the Cochlea: Linear Approximation*, J Acoust Soc Am **93**, 3320 (1993).
13. S. T. Neely and D. O. Kim, *A Model for Active Elements in Cochlear Biomechanics*, J Acoust Soc Am **79**, 1472 (1986).
14. J. E. Gale and J. F. Ashmore, *Charge Displacement Induced by Rapid Stretch in the Basolateral Membrane of the Guinea-Pig Outer Hair Cell*, Proc Biol Sci **255**, 243 (1994).
15. S. X. Sun, B. Farrell, M. S. Chana, G. Oster, W. E. Brownell, and A. A. Spector, *Voltage and Frequency Dependence of Prestin-Associated Charge Transfer*, J Theor Biol **260**, 137 (2009).
16. C. D. Geisler and X. Shan, *A Model for Cochlear Vibrations Based on Feedback from Motile Outer Hair Cells*, in *The Mechanics and Biophysics of Hearing*, edited by P. Dallos, C. D. Geisler, J. W. Matthews, M. A. Ruggero, and C. R. Steele (Springer, New York, NY, 1990), pp. 86–95.

17. J. Santos-Sacchi and W. Tan, *Complex Nonlinear Capacitance in Outer Hair Cell Macro-Patches: Effects of Membrane Tension*, Sci Rep **10**, 6222 (2020).
18. R. Nobili and F. Mammano, *Biophysics of the Cochlea. II: Stationary Nonlinear Phenomenology*, J Acoust Soc Am **99**, 2244 (1996).
19. J. Santos-Sacchi and L. Song, *Chloride-Driven Electromechanical Phase Lags at Acoustic Frequencies Are Generated by SLC26a5, the Outer Hair Cell Motor Protein*, Biophys J **107**, 126 (2014).
20. A. N. Temchin, N. C. Rich, and M. A. Ruggero, *Threshold Tuning Curves of Chinchilla Auditory-Nerve Fibers. I. Dependence on Characteristic Frequency and Relation to the Magnitudes of Cochlear Vibrations*, J. Neurophysiol. **100**, 2889 (2008).
21. A. M. Taberner and M. C. Liberman, *Response Properties of Single Auditory Nerve Fibers in the Mouse*, J Neurophysiol **93**, 557 (2005).
22. M. C. Liberman, *Auditory-nerve Response from Cats Raised in a Low-noise Chamber*, The Journal of the Acoustical Society of America **63**, 442 (1978).
23. J. Ge, J. Elferich, S. Dehghani-Ghahnaviyeh, Z. Zhao, M. Meadows, H. von Gersdorff, E. Tajkhorshid, and E. Gouaux, *Molecular Mechanism of Prestin Electromotive Signal Amplification*, Cell **184**, 4669 (2021).
24. N. Bavi, M. D. Clark, G. F. Contreras, R. Shen, B. G. Reddy, W. Milewski, and E. Perozo, *The Conformational Cycle of Prestin Underlies Outer-Hair Cell Electromotility*, Nature **600**, 7889 (2021).